



Quantitative Structure- Activity Relationship, Molecular docking, Drug- likeness and ADMET Studies of 1, 9- Diheteroarylnona- 1, 3, 6, 8- Tetraen- 5 ones Derivatives as Cancer Therapeutic Agents.

Abdulrahman Ibrahim Kubo^{1*}, Shinggu D. Yamta¹, Anthony E. Aiwonegbe², Chika Attama¹, Saminu M.A¹

¹Department of Pure and Applied Chemistry, Adamawa State University, Mubi, Nigeria

²Department of Chemistry, Faculty of Physical Sciences, University of Benin, Benin City, Nigeria

Corresponding Author Email: abdulrahmankuboibrahim@gmail.com

Received 21 Oct 2025,

Revised 13 Nov 2025,

Accepted 19 Nov 2025

Keywords:

- ✓ QSAR
- ✓ ADMET
- ✓ LNCap
- ✓ Prostate cancer
- ✓ Drug- likeness

Citation: Kubo A.I., Yamta S.D., Aiwonegbe A.E., Chika C. Saminu M.A. (2025). Quantitative Structure-Activity Relationship, Molecular docking, Drug-likeness and ADMET Studies of 1,9-Diheteroarylnona-1,3,6,8-Tetraen-5 ones Derivatives as Cancer Therapeutic Agents, *J. Mater. Environ. Sci.*, 16(12), 2235-2247.

Abstract: Cancer remains one of the most critical global health challenges, with its associated mortality rates significantly expanding. In developed countries, it accounts for over 20% of all deaths, underscoring its substantial impact. Among men, prostate cancer is a major concern, ranking as the most frequently diagnosed cancer and the second leading cause of cancer-related deaths, after lung cancer. To address this, a Quantitative Structure-Activity Relationship (QSAR) model was developed to identify potent anti-prostate cancer agents targeting the LNCap cell line. Model number one demonstrated strong reliability with the following statistical parameters of $R^2 = 0.9783$, $R^2_{adj} = 0.9674$, $SEE = 0.0632$, $Q^2 (LOO) = 0.9467$, $MAE = 0.0623$, and $CCC = 0.8682$. Molecular docking studies further supported the model predictions, identifying three top compounds with binding affinities ranging from (-9.1 to -9.4 kcal/mol) suggesting their potential as androgen receptor inhibitors. The model highlighted key molecular descriptors associated with anticancer activity: MATS5i, P1v, RDF12Ou, AATS5m, and MATS7i. This research offers valuable insights into the correlation between structural features of 1, 9- diheteroarylnona- 1, 3, 6, 8- tetraen- 5 ones compounds, their drug-likeness, and ADMET properties, contributing to the development of effective treatments for prostate cancer LNCap cell line. These findings demonstrate the potential of the developed QSAR model and docking studies to guide the design of novel and effective anti-prostate cancer agents.

1. Introduction

Cancer remains one of the most critical global health challenges, with its associated mortality rates significantly expanding (Torre *et al.*, 2015). Cancer accounts for approximately 13% of global deaths each year, making it one of the leading causes of mortality worldwide (Mahdy *et al.*, 2020). In developed countries, it accounts for over 20% of all deaths, underscoring its substantial impact. Among men, prostate cancer is a major concern, ranking as the most frequently diagnosed cancer and the second leading cause of cancer-related deaths, after lung cancer (American cancer society 2014). Among the various approaches to cancer treatment, inhibiting angiogenesis the formation of new blood vessels has emerged as a promising strategy to halt tumor progression (Robert S. Kerbel 2000). Significant efforts have been directed toward the treatment and prevention of prostate cancer (PC). While there are effective therapies for localized prostate cancer, the management of advanced or metastatic forms of the disease remains a major challenge. Standard treatment options for localized

prostate cancer (PC) include surgery and radiation therapy, either individually or in combination. These are often followed by hormonal therapy. In contrast, for advanced stage prostate cancer, the primary approach involves hormone deprivation therapy, which may also be supplemented by surgery and/or radiation (LA Robles *et al.*, 2012; van den bergh *et al.*, 2013). Historically, drug discovery has relied heavily on random screening and empirical observations of the effects of natural compounds on various diseases. Although this traditional method is inadequate, it has nonetheless contributed to the identification of several essential therapeutic agents. However, this approach is time consuming, labor intensive and expensive (Leelananda & Lindert 2016).

Computer-aided drug design (CADD), which utilizes molecular modeling techniques, was employed to enhance the efficiency of developing new drugs by using *in silico* simulations. Molecular modeling allows for the rapid assessment of numerous compounds, helping to understand how they interact with pharmacologically relevant targets before they are synthesized. This approach enables the prediction and analysis of critical properties such as toxicity, biological activity, bioavailability, and overall effectiveness prior to *in vitro* testing, thereby facilitating more strategic and informed experimental planning (Ferreira & Glaucious 2011; Ouahhoud *et al.*, 2022). Molecular docking, a key component of this process, investigates the interactions between molecular structures for example, how a drug molecule fits and binds to a protein receptor or enzyme. Molecular docking software is widely used in drug design, with one of its primary applications being virtual screening. This computational approach provides valuable insights into the molecular interactions, such as hydrogen bonding, hydrophobic contacts, and electrostatic forces, that stabilize the ligand–receptor complex. This technique identifies promising candidates from a molecular database for further investigation. As such, a reliable and rapid computational method is essential (Yang *et al.*, 2011; Diass *et al.*, 2023; Louati *et al.*, 2025). This study aim at building a QSAR model on a series of 1, 9- diheteroarylnona-1, 3, 6, 8- tetraen- 5 -one derivatives as potential inhibitors associated with prostate cancer. The research also involves molecular docking studies, evaluating their drug-likeness and ADMET properties (Ridal *et al.*, 2026).

2. Methodology

2.1 Materials

The entire research was conducted using an HP EliteBook laptop equipped with a dual-core Intel CPU running at 2.5 GHz and 4.0 GB of RAM, operating on the Windows 8. The following software packages were employed throughout the study: ChemDraw v12.1, Spartan 14 v1.1.0, PyRx Docking Software, and Discovery Studio. Additionally, the SwissADME and ADMET lab 2.0 online tools were utilized to evaluate the drug-likeness and ADMET properties of the compounds under investigation (Ridal *et al.*, 2026).

2.2 Selection of molecules

A series of 1, 9- diheteroarylnona-1, 3, 6, 8- tetraen- 5 - one derivatives were gotten from the work of Zhang and colleagues (Zhang *et al.*, 2016) for the purpose of this study. All compounds were evaluated against the LNCaP prostate cancer cell line.

2.3 Transformation of 2D to 3D and geometry optimization

The 2D structures of 1, 9- diheteroarylnona-1, 3, 6, 8- tetraen- 5 - one derivative were initially drawn using ChemDraw v12.1, after which they were converted into 3D models for geometry optimization. This was achieved through Density Functional Theory (DFT) quantum mechanical calculations using

Spartan 14 v1.1.0 software (Al Hamzi *et al.*, 2012; Al Hamzi *et al.*, 2012;). The B3LYP functional and the 6-31G* basis set were applied to determine the most stable conformations of the molecules. The optimized structures were subsequently saved in PDB format in a dedicated file (El Aoufir *et al.*, 2016; Yunusa *et al.*, 2021; Abdulrahman & Ibrahim 2024; Kadda *et al.*, 2025; Kubo A.I *et al.*, 2026).

2.4 Model development

For internal validation, the predictive models were assessed using several statistical metrics in DTC Lab software (https://teqip.jdvu.ac.in/QSAR_Tools/): the coefficient of determination (R^2), the adjusted coefficient of determination (R^2_{adj}), the standard error of estimation (SEE), leave one out Q^2 (LOO) and the mean absolute error (MAE). While these metrics are necessary, they are not sufficient on their own to confirm model robustness. Therefore, additional validation was conducted using the Variance Inflation Factor (VIF), which quantifies the level of multicollinearity among the descriptors in the regression model. The VIF is calculated as follows:

$$VIF = \frac{1}{(1-R^2)} \quad (1)$$

R^2 is the correlation coefficient, the higher the value, the larger the link between the model parameters. The VIF values below 10 shows the equation is stable while the values above 10 signify the equation is not efficient and cannot be employed (Myers 1990). The contribution of each descriptor in the selected model was assessed using the mean effect (M/E) value of each descriptor. This mean effect reflects how each descriptor influences the resulting equation. The sign of each model parameter indicates whether the descriptor contributes positively or negatively to the overall equation (Minovski *et al.*, 2013). This relationship is expressed as follows:

$$Mean\ Effect = \frac{\beta_j \sum_i^n D_j}{\sum^m (\beta_j \sum_i^n D_j)} \quad (2)$$

Where m equals the model parameters, β_j equals to descriptors coefficient j , n equals to the prediction set molecules and D_j is the matrix value of the model parameter in the prediction set.

To externally validate the developed model, a test set was used, by evaluating the value of Concordance Correlation Coefficient (CCC) in the DTC Lab software. For the model to be considered reliable, the (CCC) value should exceed 0.8. This is expressed as:

$$CCC = \frac{2 \sum_{i=1}^{n_{EXT}} (Y_i - \bar{Y})(Y_i - \bar{Y}_i)}{\sum_{i=1}^{n_{EXT}} (Y_i - \bar{Y})^2 + \sum_{i=1}^{n_{EXT}} (Y_i - \bar{Y}_i)^2 + n_{EXT} (Y_i - \bar{Y}_i)^2} \quad (3)$$

Y_i is the experimental value, \bar{Y} is the average of experimental value, \bar{Y}_i is the predicted value of activity and \bar{Y}_i is average of the predicted value of the activity. EXT is the external prediction set or test set (Chirico & Gramatica 2011).

2.5 Protein download and preparation

The crystal structure of the target protein was retrieved from the Protein Data Bank (PDB ID: 4r0l) via the RCSB website (<https://www.rcsb.org/>) (LV. H *et al.*, 2015). The structure was then imported into the Discovery Studio Software workspace for preparation, where any structural errors in the amino acid residues were corrected.

2.6 Molecular docking process

The PyRx docking software was employed to perform ligand- protein docking in this study. Before initiating the docking process, the prepared protein structure was imported into the PyRx workspace. Similarly, the optimized ligands were imported into the software, and docking simulations were conducted. The docking scores and binding affinities were analyzed to identify the most stable ligand–receptor complexes (Alshahateet, *et al.*, 2024; Merzouki, *et al.*, 2024). Various intermolecular interactions, including hydrogen bonding, and hydrophobic interactions were visualized using Discovery Studio software. The target protein receptor is believed to influence the efficacy and potency of the proposed compounds as potential anticancer agents (Kubo AI *et al.*, 2024).

2.7 ADMET and drug-likeness properties

Accessible online web servers such as swissADME and ADMET lab 2.0 were utilized to assess the drug-likeness and ADMET (Absorption, Distribution, Metabolism, Excretion, and Toxicity) profiles of the investigated compounds in this study (Abbaoui, *et al.*, 2024). These tools assist researchers in identifying viable drug candidates, reducing the need for extensive experimental procedures, and improving the overall success rate of drug development. They provide valuable insights into pharmacokinetic and physicochemical parameters such as solubility, permeability, and metabolic stability. In this study, Lipinski's Rule of Five was applied as the initial screening criterion for drug-likeness, followed by the evaluation of key ADMET properties that reflect the pharmacokinetic behavior of the candidate molecules.

3. Results and Discussion

3.1 QSAR Results

This study focuses on developing a quantitative structure- activity relationship (QSAR) model to predict the biological activities of 1, 9- diheteroarylnona-1, 3, 6, 8-tetraen-5- one derivatives as potential inhibitors of LNCap prostate cancer cell line. Molecular docking study was carried out as well as evaluation of the compounds drug- likeness and ADMET properties. The Kennard- Stone algorithm was employed to divide the dataset into training (model building) and test (validation) sets, facilitating an accurate assessment of model performance. Using the Genetic Function Algorithm (GFA), a model was generated, and was identified as robust based on its statistical metrics:

$R^2 = 0.9783$, R^2 (Adjusted) = 0.9674, Standard Error of Estimation (SEE) = 0.0632, Q^2 (LOO) = 0.9467, Mean Absolute Error (MAE) = 0.0623, CCC = 0.8682

$pIC_{50} = 15.0388, (*MAT5i) +1.5311, (*P1v) +20.5971, (*RDF120u) +0.0726, (*AATS5m) +0.0058, (*MAT7i) +6.9432.$ (4)

The model contains 2D atoms pairs at various topological distances: (AATS5m) defined as Average Broto- Moreau autocorrelation- lag 5/ weighted by mass which is used in the model to measure the distribution of atomic properties on the molecule topology. (MAT5i) defined as Moran autocorrelation- lag 5/ weighted by first ionization potential. (MAT7i) defined as Moran autocorrelation- lag 7 weighted by first ionization potential which is used in the model to measure spatial distribution of environmental properties. These descriptors especially those related to ionization potential highlight the relevance of hydrogen bonding between atom pairs separated by five and seven bonds (lags 5 and 7) in influencing the biological activity of the 1, 9-diheteroarylnona-1, 3, 6, 8- tetraen-5- one derivatives against the prostate cancer LNCap cell line.

The model also contain 3D atom type (P1v) defined as 1st component shape directional WHIM index/ weighted by relative van der waals volume. This is geometrical descriptor based on statistical indexes calculated on the projection of the atoms along principal axes. (RADF120u) is defined as Radial distribution function- 120/ unweighted. The molecular descriptors AATS5m, MATS5i, MATS7i, P1v and RADF120u plays a crucial role in the development of the model and exhibit a strong positive influence on the activity of 1, 9 -diheteroarylnona-1, 3, 6, 8-tetraen-5- one derivatives. These findings indicate that the descriptors used in constructing the model are relevant and effective. **Table 1** presents the observed and predicted pIC₅₀ values, residuals, and docking scores for the compounds under study. **Table 2** displayed definitions and classifications of the descriptors used in Model 1. To further evaluate the impact and inter-correlation of the descriptors, additional statistical analysis was conducted, and the results are shown in **Table 3**.

The Y-randomization test results (**Table 4**) confirm the models robustness, showing low values for R² and Q²- Loo, which suggest the absence of chance correlation. **Figure 1** displays a scatter plot of standardized residuals versus observed activities, highlighting the models predictive strength. **Figure 2** illustrates a scatter plot comparing experimental biological activity with predicted values, with a distribution for substances on both sides of zero. This suggests that no systematic error is present in the developed model. Therefore, the model is considered accurate, reliable, and robust.

Table 1. Observed, Predicted, Residual and Docking score of model 1

S/No	Observed pIC ₅₀	Predicted pIC ₅₀	Residuals	Docking Score (Kcal/mol)
*1.	5.1643	4.9142	-0.2500	-6.5
2.	5.0963	5.1210	0.0246	-7.0
3.	5.0920	4.9632	-0.1287	-6.5
4.	5.5883	5.5736	-0.0147	-7.3
5.	5.2118	5.2535	0.0417	-6.5
6.	5.3477	5.3051	-0.0426	-6.6
7.	5.6143	5.6066	-0.0077	-5.4
*8.	5.2502	5.1094	-0.1408	-6.4
*9.	4.7562	5.5362	0.7799	-7.4
10.	5.2182	5.2036	-0.0146	-7.7
11.	5.3062	5.4077	0.1015	-7.5
12.	5.2298	5.2661	0.0363	-8.3
13.	5.7878	5.7513	-0.0364	-7.2
14.	5.6635	5.6768	0.0133	-7.1
15.	4.8658	4.9039	0.0381	-9.1
16.	4.7652	4.8004	0.0352	-6.4
*17.	6.0087	4.8269	-1.1818	-8.7
18.	6.0132	6.0334	0.0201	-9.4
19.	5.8268	5.8045	-0.0222	-7.8
*20.	5.4377	5.1005	-0.3371	-7.8
*21.	5.5228	5.6420	0.1191	-9.2
22.	5.3655	5.3216	-0.0438	-8.0
23.	5.2162	5.3076	0.0914	-7.0
24.	5.1820	5.5632	0.3812	-7.5
25.	4.5652	4.8004	0.2352	-8.2

*Denote test set

Table 2. Definition of descriptors and their class for model

Name	Definition	Class
MATS5i	Moran Autocorrelation- lag 5/ weighted by first ionization potential	2D
P1v	1 st component shape directional WHIM index/ weighted by relative Van der waals volume	3D
RDF120u	Radial distribution function- 120/ unweighted	3D
AATS5m	Average Broto- Moreau autocorrelation- lag 5/ weighted by mass	2D
MATS7i	Moran autocorrelation- lag 7/ weighted by first ionization potential	2D

Table 3. Statistical analysis of model 1 parameters

	<i>MATS5i</i>	<i>P1v</i>	<i>RDF120u</i>	<i>AATS5m</i>	<i>MATS7i</i>	<i>VIF</i>	<i>M/E</i>
MATS5i	1	0.2016	-0.5672	0.1309	-0.1227	1.5157	-0.0011
P1v	0.2016	1	-0.2921	-0.4898	-0.2738	1.9949	0.0159
RDF120u	-0.5672	-0.2921	1	-0.0759	0.1341	1.5866	0.1114
AATS5m	0.1309	-0.4898	-0.0759	1	-0.2569	1.8525	0.8737
MATS7i	-0.1227	-0.2738	0.1341	-0.2569	1	1.3905	1.3446

Table 4. Y- Randomization Test

MODEL TYPE	R ²	Q ² -LOO
ORIGINAL	0.9783	0.9467
Random 1	0.3901	-0.3814
Random 2	0.3448	-0.7087
Random 3	0.1296	-1.1562
Random 4	0.3496	-0.8033
Random 5	0.0865	-1.46
Random 6	0.2873	-0.8220
Random 7	0.2383	-1.0826
Random 8	0.4442	-0.5726
Random 9	0.3949	-0.4840
Random 10	0.1516	-1.2875
Summary		
R ²	(Original Model)	0.9783
Q ² -LOO	(Original Model)	0.9467
Average R ²	(10 Random Models)	0.2817
Average Q ² -LOO	(10 Random Models)	-0.8758

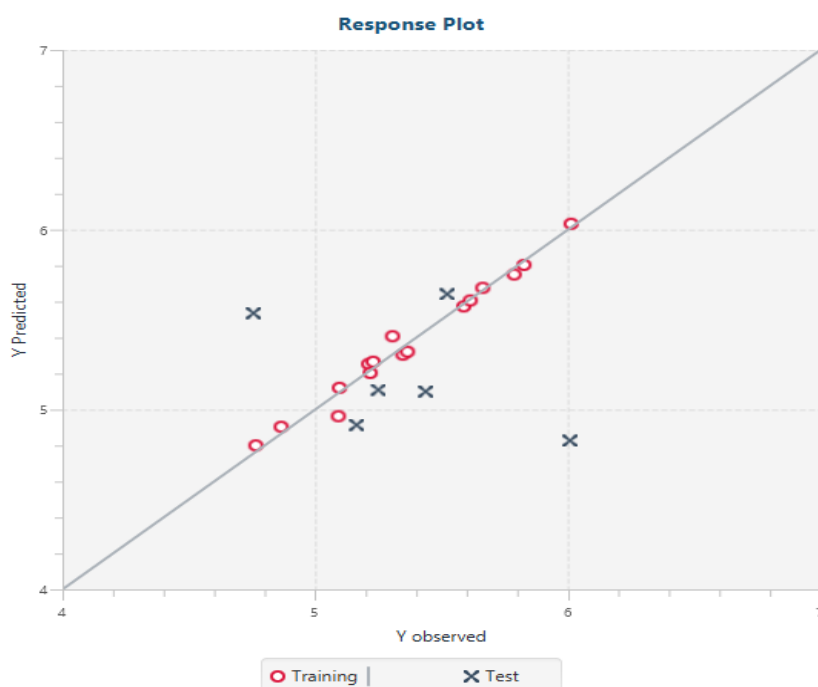


Figure 1: Scatter plot of standardized residual versus the Investigational activities

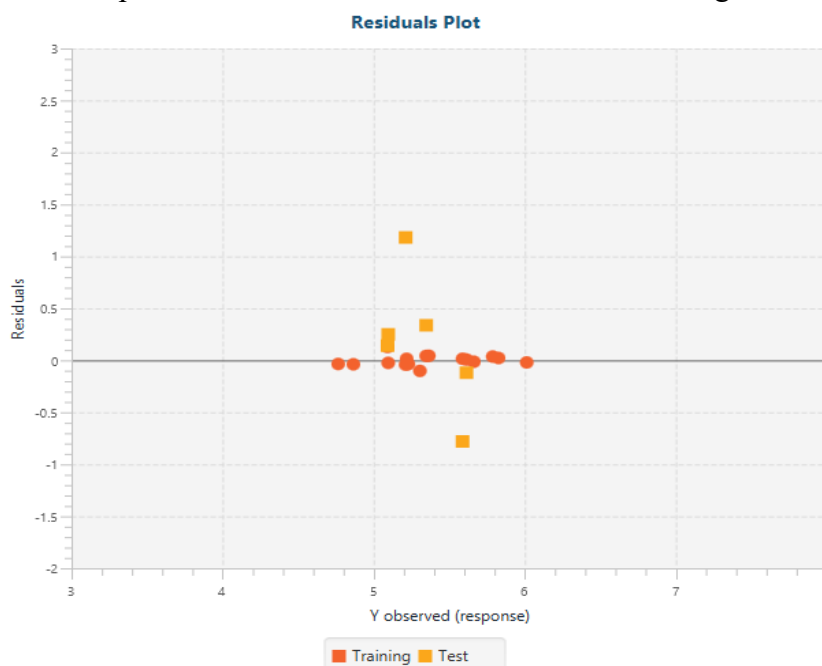


Figure 2: Scatter plots of biological activities against calculated activities

3.2 Docking Result

Molecular docking simulations were carried out on a series of 1, 9-diheteroarylnona-1, 3, 6, 8-tetraen-5-one derivatives against the binding site of the protein receptor (PDB ID: 4r0l). PyRx docking software was utilized for this purpose, as it is known to deliver more accurate and reliable results compared to other docking software. Compounds 18, 21, and 15 emerged as promising hit candidates based on their superior docking scores, ranging from (-9.1 to -9.4 kcal/mol) respectively. The docking scores for all the compounds are displayed in [Table 1](#). Detailed interaction profiles between the potential hit compounds and the 4r0l protein receptor, including hydrogen bonding and Pi-related interactions with various amino acid residues, are provided in [Table 5](#). In case of hydrogen bonding, the distances are also specified.

Compound 18 has the highest docking score (-9.4 kcal/mol) formed two conventional hydrogen bonds with SER214 at a distance of (5.12 Å) and TRP141 at a distance of (5.88 Å). Additionally, it engaged in a Pi- sigma interaction with HIS40 at a distance of (4.60 Å). It also exhibited two amide-Pi stacking interactions with CYS191 at a distance of (6.32 Å), (5.16 Å) and two with TRP215 at a distance of (7.14 Å) and (6.50 Å) respectively. Both 3D and 2D visual representations of compound 18 bonds to the receptor are shown in **Figure 3**.

Compound 21 with a docking score of (-9.2 kcal/mol) formed two conventional hydrogen bonds with TRP141 at a distance of (5.61 Å) and SER214 at a distance of (5.24 Å). A Pi- sigma interaction was also observed with GLY151 at a distance of (3.83 Å). Moreover, the compound exhibited two amide- Pi stacking interactions with TRP215 at a distance of (6.54 Å) and CYS191 at a distance of (5.07 Å) and (6.32 Å), along with a Pi- alkyl interaction involving CYS220 at a distance of (6.77 Å) respectively. The 3D and 2D binding conformations of compound 21 are displayed in **Figure 4**.

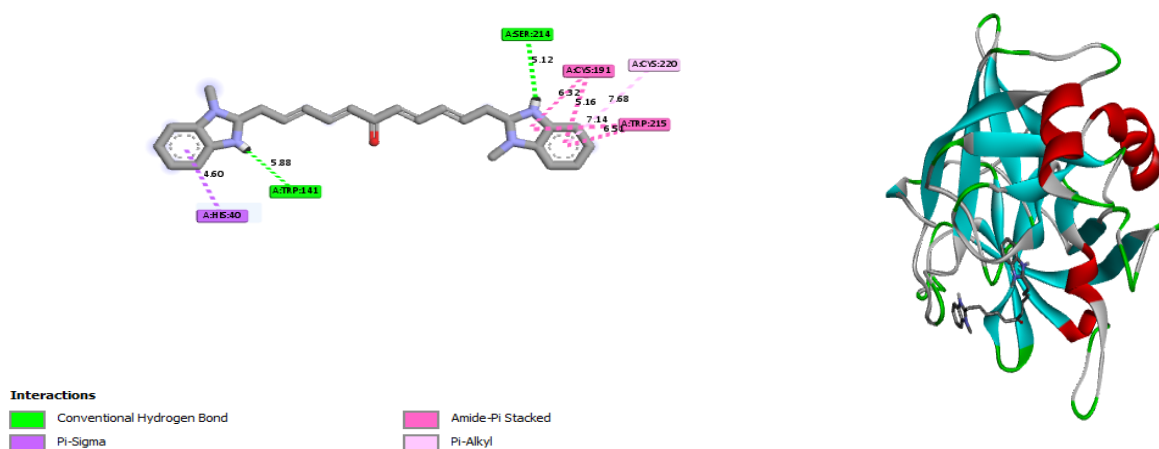


Figure 3: 3D and 2D representations of the compound18 in the active site of the 4r0l receptor

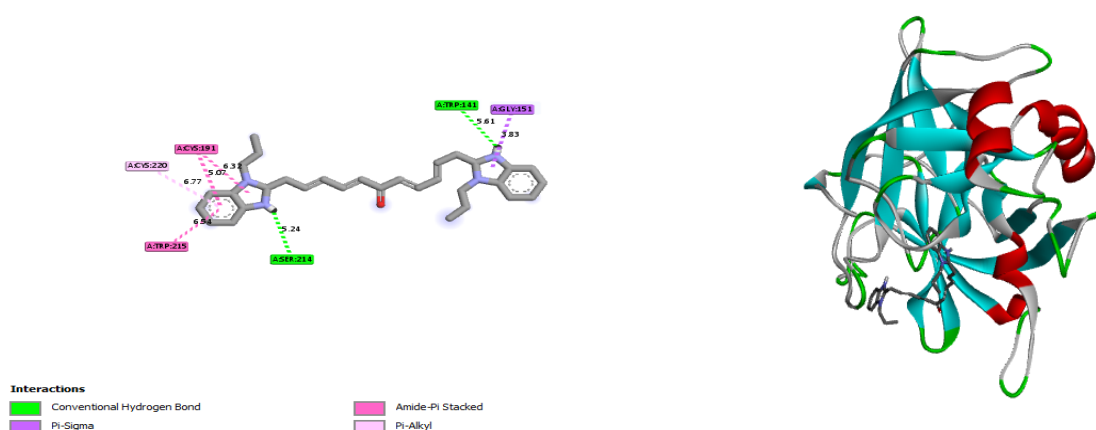


Figure 4: 3D and 2D representations of the compound 21 in the active site of the 4r0l receptor

Compound 15 with binding score of (-9.1 kcal/mol) interacted with the 4r0l receptor through Pi- Pi T-shaped interactions with TRP215 at a distance of (6.74 Å) and CYS191 at a distance of (5.06 Å). Additionally, it formed an amide- Pi stacked interaction with HIS34 at a distance of (7.30 Å) and Pi- alkyl interactions with CYS220 at a distance of (7.65 Å) and HIS40 at a distance of (4.46 Å). 3D and 2D interaction visualizations of compound 15 within the active site of the receptor is shown in **Figure 5**.

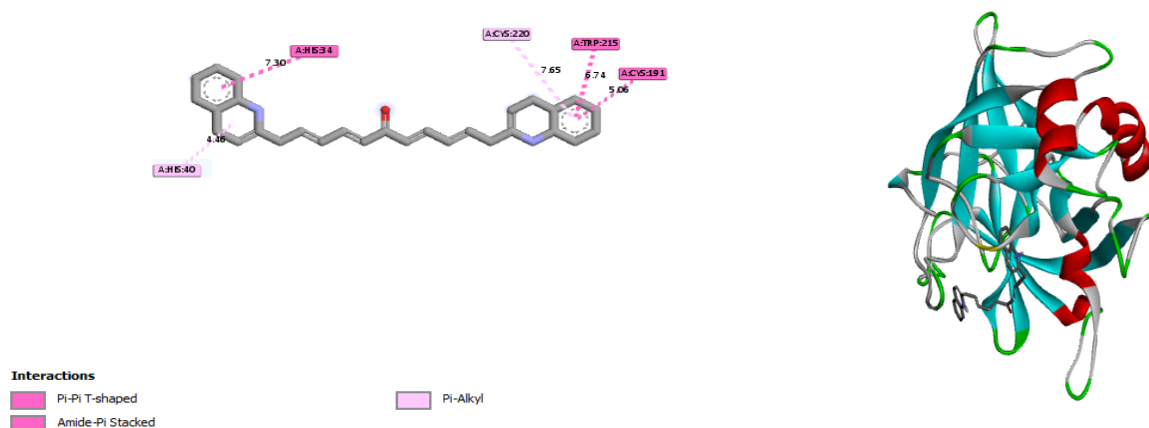


Figure 5: 3D and 2D representations of the compound 15 in the active site of the 4r0l receptor

Table 5: The results of interactions of the potential hit compounds and 4ro1 protein receptor

S/No.	H-Bond		Hydrophobic interaction
	Amino acids	Length Å	
18	SER214	5.12	SER214, TRP141, HIS40, CYS191, TRP215
	TRP141	5.88	
21	SER214	5.24	GLY151, TRP215, CYS191, CYS220
	TRP141	5.61	
15			TRP215, CYS191, HIS34, HIS40, CYS220

3.3 Drug- likeness and ADMET Results

To confirm the potential of the identified hit compounds as viable drug candidates, their ADMET profiles and drug-likeness properties were thoroughly evaluated (Merzouki, *et al.*, 2024). The online platform swissADME was employed to assess drug-likeness, while ADMET lab 2.0 was utilized to predict ADMET properties of the selected compounds (Daina *et al.*, 2017). A key criterion in early phase drug discovery is the evaluation of drug-likeness, which involves correlating molecules physicochemical characteristics with its biopharmaceutical behavior in the human body, particularly its oral bioavailability (Birketon *et al.*, 2012). The most widely recognized framework for this analysis is Lipinski's Rule of Five, which proposes that a compound is likely to be well absorbed or permeable if it satisfies the following conditions: molecular weight < 500, hydrogen bond donors (HBD) < 5, hydrogen bond acceptors (HBA) < 10. A compound is generally considered drug like if it does not violate more than two of these rules (Christopher *et al.*, 1997). The drug-likeness analysis results, displayed in Table 6, reveal that all selected hit compounds are well absorbed, permeable, and demonstrate favorable drug-likeness profiles. Additionally, bioavailability scores were calculated, with all compounds achieving a value of 0.55, indicating a strong likelihood of optimal permeability and bioavailability and further confirming compliance with Lipinski's rules (Martin YC 2005).

The compounds were also assessed for synthetic accessibility, which estimates how easily a compound can be synthesized, based on a scale that ranges from 1 (very easy to synthesize) to 10 (very difficult). The selected compounds scored between 3.59 and 4.05 (Table 6), suggesting they are relatively easy to synthesize. Further ADMET profiling was conducted to examine metabolic stability and other pharmacokinetic properties (Table 7). The results indicate that the hit compounds exhibit favorable ADMET characteristics. They function both as substrates and inhibitors of cytochrome P450

enzymes, which are crucial for drug metabolism, and are predicted to be efficiently eliminated from the body, supporting their potential as drug candidates.

Table 6: Results of the drug-likeness properties of the potential hit compounds

S/No	MW	HBA	HBD	Synthetic Accessibility	Bioavailability Score	Lipinski Violation	Drug-likeness
18	422.52	3	0	3.59	0.55	0	YES
21	478.63	3	0	4.05	0.55	0	YES
15	416.51	3	0	4.01	0.55	0	YES

Table 7: Selected ADMET properties of the inhibiting compounds

Properties	Compound 18	Compound 21	Compound 15
Absorption			
PgP- Inhibitor	low probability	low probability	low probability
PgP- Substrate	low probability	low probability	low probability
Human Intestinal absorption	07% probability	08% probability	05% probability
Distribution			
BBB penetration	Low	Low	Low
Metabolism			
CYP1A2 inhibitor	Moderate	Moderate	High
CYP1A2 substrate	High	Low	Low
CYP2C19 inhibitor	Moderate	High	High
CYP2C19 substrate	Low	Low	Moderate
CYP2C9 inhibitor	Moderate	High	High
CYP2C9 substrate	High	High	High
CYP2D6 inhibitor	High	High	High
CYP2D6 substrate	High	High	High
CYP3A4 inhibitor	High	High	High
CYP3A4 substrate	Moderate	High	Low
Excretion			
Clearance (ML/Min/Kg)	3.88	4.434	2.035
T ^{1/2}	Short	Short	Short
Toxicity			
AMES toxicity	Low probability	Low probability	Low probability
Skin sensitization	Low probability	Low probability	Low probability
Carcinogenicity	Low probability	Low probability	Low probability
Eye irritation	Low probability	Low probability	Low probability
Respiratory toxicity	Low probability	Low probability	Low probability

Conclusion

Molecular docking was conducted on a series of 1, 9- diheteroarylnona-1, 3, 6, 8- tetraen-5-one derivatives to evaluate their potential as inhibitors of the 4r0l receptor using PyRx software. Three compounds demonstrated better docking scores and were selected as potential hit candidates for further investigation. Subsequently, these hit compounds were evaluated for their drug-likeness and pharmacokinetic properties through ADMET and drug-likeness analyses. A bioavailability score of 0.55 indicated that the compounds are likely to be orally bioavailable, while their synthetic accessibility

scores, ranging from 3.59 to 4.05, suggest they are relatively easy to synthesize. Moreover, ADMET analysis showed favorable pharmacokinetic behavior. The compounds were predicted to act as both substrates and inhibitors of cytochrome P450 enzymes, which are vital in drug metabolism, and were also found to be readily eliminated from the body, supporting their potential as promising drug candidates.

Declaration of interest statement: Authors declare no conflict of interest.

Authors' contribution: The authors contributed equally in drafting the manuscript

References

- Abbaoui, Z., Merzouki, M., Oualdi, I., Bitari, A., Oussaid, A., Challioui, A., ... & Diño, W. A. (2024). Alzheimer's disease: In silico study of rosemary diterpenes activities. *Current Research in Toxicology*, 6, 100159.
- Abdulrahman Ibrahim Kubo & Ibrahim Birma Bwatanglang (2024). QSAR, Molecular docking studies and Pharmacokinetics properties prediction of some thiosemicarbazone derivatives containing indole fragments targeting prostate cancer cell. *IRJIET*, 8, issue 8, 156-166. <https://doi.org/10.47001/IRJIET/2024.808417>.
- Al Hamzi A. H., Zarrok, H. Zarrouk A., Salghi R., *et al.* (2013), The Role of Acridin-9(10H)-one in the Inhibition of Carbon Steel Corrosion: Thermodynamic, Electrochemical and DFT Studies, *Int. J. Electrochem. Sci.*, 8 N°2, 2586-2605, [https://doi.org/10.1016/S1452-3981\(23\)14334-3](https://doi.org/10.1016/S1452-3981(23)14334-3)
- Alshahateet, S. F., Altarawneh, R. M., Al-Tawarh, W. M., Al-Trawneh, S. A., Al-Taweel, S., Azzaoui, K., ... & Jodeh, S. (2024). Catalytic green synthesis of Tin (IV) oxide nanoparticles for phenolic compounds removal and molecular docking with EGFR tyrosine kinase. *Scientific reports*, 14(1), 6519.
- American Cancer Society (2014). Cancer facts and figures, Atlanta: American cancer society, 2014.
- Birketon GR., Paolini GV., Besnard J., Muresan S., Hopkins AL., (2012). Quantifying the beauty of Drugs. *Nat Chem* 4(2), 90- 8. [Doi:10.1038/nchem.1243](https://doi.org/10.1038/nchem.1243).
- Bouammali, H., Zraibi, L., Ziani, I., Merzouki, M., Bourassi, L., Fraj, E., Challioui, A., Azzaoui, K., Sabbahi, R., Hammouti, B., *et al.* (2024). Rosemary as a Potential Source of Natural Antioxidants and Anticancer Agents: A Molecular Docking Study. *Plants*, 13, 89. <https://doi.org/10.3390/plants13010089>
- Chirico N., Gramatica P (2011). Real external predictivity of QSAR models: how to evaluate it? Comparison of different validation criteria and proposal of using concordance correlation Coefficient. *J Chem. Inf model.* 51(9), 2320- 35. [Doi:10.21/ci200211n](https://doi.org/10.21/ci200211n).
- Christopher A. Lipinski., Franco Lombardo., Beryl W. Dominy., Paul J. Feeney (1997). Experimental and computational approaches to estimate solubility and permeability in drug discovery and development settings, *Advanced Drug delivery Review*, 23, Issue 1-3, 3-25. [https://doi.org/10.1016/S0169-409X\(96\)00423-1](https://doi.org/10.1016/S0169-409X(96)00423-1).
- Daina A., Michielin O., Zoete V (2017). swissADME: a free web tool to evaluate pharmacokinetics, drug-likeness and medicinal chemistry friendliness of small molecules. *Sci. Rep.* 7, 42717. [Doi:10.1038/srep42717](https://doi.org/10.1038/srep42717).
- Diass K., Merzouki M., El Fazazi K., Azzouzi H., Challioui A., Azzaoui K., Hammouti B., Touzani R., Depeint F., Ayerdi-Gotor A., Rhazi L. (2023). Essential oil of *Lavandula officinalis*: Chemical composition and antibacterial activities, *Plants*, 12, 1571. <https://doi.org/10.3390/plants12071571>
- EL Aoufir Y., Lgaz H., Bourazmi H., Kerroum Y., Ramli Y., Guenbour A., Salghi R., El-Hajjaji F., Hammouti B., Oudda H. (2016), Quinoxaline Derivatives as Corrosion Inhibitors of Carbon Steel in Hydrochloric Acid Media: Electrochemical, DFT and Monte Carlo simulations studies, *J. Mater. Environ. Sci.*, 7 (12), 4330-4347
- Ferreira RS., Glaucious O (2011). Integrating virtual and high-throughput screening: opportunities

- And challenges in drug research and development *Quim. Nova* 34(10), 1770- 1778. [https://Doi.org/10.1590/S0100-40422011001000010](https://doi.org/10.1590/S0100-40422011001000010).
- Kadda S., Merzouki M., Alaloui M.M., Himri C. (2025). DFT and Docking Techniques: Bibliometric analysis, *Arab. J. Chem. Environ. Res.* 12 (2), 167-178
- Kubo AI., Uzairu A., Babalola IT., Ibrahim MT., Umar AB (2024). QSAR, molecular docking, and Pharmacokinetic analysis of thiosemicarbazone- indole compounds targeting prostate cancer Cells. *J Taibah Univ Med Sci.* 19(4), 823- 854. [Doi:10.1016/j.jtumed.2024.07.004](https://doi.org/10.1016/j.jtumed.2024.07.004)
- Kubo A.I., wafi H.G., Attama C., Aiwonegbe A.E., John J.H. and Saminu M.A. (2026) DFT- QSAR Model Generation of Pyrimidocarbazole Derivatives as Breast Cancer Inhibitors by the Genetic Algorithm and Multiple Linear Regression (GA- MLR) method, *Arab. J. Chem. Environ. Res.* 13(1), 18- 40.
- Leelananda SP., Lindert S (2016). Computational methods in drug discovery. *Beilstein J. Org. Chem.* 12, 2694-2718. [Doi:10.3762/bjoc.12.267](https://doi.org/10.3762/bjoc.12.267).
- Louafi B., Ouazzani R., Akoh R., Kadda S., Ben Hadda T., EL-Otmani N., El Ghazal A., El Mekkaoui A., Bousta D., and Benjelloun M. (2025). Optimization of Ultrasound-Assisted Extraction, Phytochemical Profiling, and Antioxidant Properties of *Ceratonia siliqua* L. Leaves Using a Mixture Design Approach: POM Theory as Guide and Sustainable Development of Agriculture, *Mor. J. Chem.*, 13(4), 2039-2067
- LA Robles., S Chou., O Cole., A Hamid., A Griffiths., K Vedhara (2012). Factors influencing patients treatment selection for localised prostate cancer: A systematic review, *British Journal of Medical and Surgical Urology*, 5, Issue 5, 207- 215, ISSN 1875- 9742, <https://doi.org/10.1016/j.bjmus.2011.11.005>.
- LV H., Zhu Y., Qiu Y., Niu L., Teng M., Li X (2015). Structural analysis of Dis312, an exosome-Independent exonuclease from *schizosaccharomyces pombe*. *Acta Crystallogr D Biol Crystallogr.* 2015 Jun; 71(Pt 6), 1284- 94. [Doi:10.1107/S1399004715005805](https://doi.org/10.1107/S1399004715005805).
- Martin YC (2005). A bioavailability score. *J Med Chem.* 48(9), 3164- 70. [Doi:10.1021/Jm0492002](https://doi.org/10.1021/Jm0492002).
- Mahdy H.M., Mohammed K. Ibrahim., Ahmed M. Metwaly., Amany Belal, Ahmed B.M. Mehany., Kamal M.A. El-Gamal, Abdou El-Sharkawy, et al. (2020) Design, synthesis, molecular modeling, in vivo studies and anticancer evaluation of quinazolin-4(3H)-one derivatives as potential VEGFR-2 inhibitors and apoptosis inducers. *Journal of Bioorganic Chemistry*, 94, 103422, ISSN 0045-2068. <https://doi.org/10.1016/j.bioorg.2019.103422>.
- Merzouki, M., Bekkouch, A., Alkowni, R., Bourassi, L., Abidi, R., Bouammali, B., ... Challioui, A. (2023). Flavone Derivatives as Potential Inhibitors of SARS-Cov-2rdrp through Computational Studies. *Journal of Biochemical Technology*, 14(4-2023), 74-82.
- Merzouki, M., Bourassi, L., Abidi, R., Bouammali, B., Sabbahi, R., Challioui, A. (2024). Deciphering the SARS-CoV-2 delta variant: Antiviral compound efficacy by molecular Docking, ADMET, and Dynamics studies. *Moroccan Journal of Chemistry*, 12(3), 1153-1171.
- Minovski N., Zuperl Š., Drgan V., Novič M (2013). Assessment of applicability domain for multivariate counter- propagation artificial neural network predictive models by minimum euclidean Distance space analysis: a case study. *Anal Chim Acta.* 759, 28-42. [Doi:10.1016/j.aca.2012.11.002](https://doi.org/10.1016/j.aca.2012.11.002).
- Myers RH (1990). *Classical and Modern Regression Application*. 2nd Edition, Duxbury Press, California USA.
- Ouahhoud S., Bencheikh N., Khoulati A., Kadda S., Mamri S., Ziani A., Baddaoui S., Eddabbeh F. E., Ellassri S., Lahmass I., Benabbes R., Addi M., Hano C., Choukri M., Bennani A., Asehraou A., Saalaoui E. (2022), *Crocus sativus* L. Stigmas, tepals, and leaves ameliorate gentamicin-induced renal toxicity: a biochemical and histopathological study, *Evidence-based Complementary and Alternative Medicine*. 2022, 13, 7127037, <https://doi.org/10.1155/2022/7127037>.
- Ridal Z., Abbaoui Z., Elmsellem H., Aouniti A., Yousfi E.B., El Kodadi M., Belkhiri C., Souna F., Touzani R., Elhenawy A.A., Hammouti B. (2026) Multifaceted Applications of Pyrazole-

Based Tetradentate Ligand Coordinated with Transition Metals (Fe, Zn, Co, Cu): Synthesis, Characterization, Catalysis, Antimicrobial Activity, ADMET, and Molecular Docking Insights, *ASEAN Journal of Science and Engineering*, 5(2), 149-172

- Robert S. Kerbel (2000). Tumor angiogenesis: past, present and the near future, *Carcinogenesis*, 21, Issue 3, 505- 515. <https://doi.org/10.1093/carcin/21.3.505>.
- Torre LA., Bray F., Siegel RL., Ferlay J., Lortet- Tieulent J., Jemal A (2015). Global cancer statistics 2012. *CA Cancer J Clin.* (2015) Mar; 65(2):87- 108. [Doi:10.3322/caac.21262](https://doi.org/10.3322/caac.21262).
- van den Bergh RC., Albertsen PC., Bangma CH., Freedland SJ., Graefen M., Vickers A., van derPoel HG (2013). Timing of curative treatment for prostate cancer: a systematic review. *Eur Urol.* 2013 Aug;64(2):204- 15. [Doi:10.1016/j.eururo.2013.02.024](https://doi.org/10.1016/j.eururo.2013.02.024).
- Yang Y., Qin J., Liu H., Yao X (2011). Molecular dynamics simulation, free energy calculation and Structure based 3D- QSAR studies of B- RAF kinase inhibitors. *J Chem Inf Model.* (2011) Mar 28;51(3):680- 92. [Doi:10.1021/ci100427j](https://doi.org/10.1021/ci100427j).
- Yunusa U., Umar U., Idris S., Kubo A., Abdullahi T (2021). Experimental and DFT Computational Insights on the Adsorption of Selected Pharmaceuticals of Emerging Concern from water system onto magnetically modified Biochar. *JOTCSA*, 8(4), 1179-1196 <https://doi.org/10.18596/jotcsa.9001197>.
- Zhang X., Wang R., Perez GR., Cheng G., Zhang Q., Zheng S., Wang G., Chen QH. (2016) Design Synthesis and biological evaluation of 1, 9- diheteroarylnona- 1, 3, 6, 8- tetraen- 5- ones as a New class of anti- prostate cancer agents. *Bioorg Med Chem.* 24(19), 4692-4700. [Doi:10.1016/j.bmc.2016.08.006](https://doi.org/10.1016/j.bmc.2016.08.006).

(2025); <http://www.jmaterenvirosci.com>